Cement & Concrete Composites 38 (2013) 50–56

Contents lists available at SciVerse ScienceDirect

Cement & Concrete Composites

journal homepage: www.elsevier.com/locate/cemconcomp

Production and properties of foamed reservoir sludge inorganic polymers

Kun-Hsien Yang, Chia-Wei Lo, Jong-Shin Huang *

Department of Civil Engineering, National Cheng Kung University, Tainan 70101, Taiwan, ROC

ARTICLE INFO

Article history:
Received 28 September 2012
Received in revised form 20 March 2013
Accepted 22 March 2013
Available online 30 March 2013

Keywords:
Foam
Reservoir sludge
Inorganic polymer
Alkali-activation

ABSTRACT

The feasibility of using reservoir sludge as a raw material in the production of foamed inorganic polymers with different densities is investigated in this work. Reservoir sludge is first crushed, ground down and then calcined at the temperature of 850 °C for 6 h to become calcined reservoir sludge (CRS) powders. A mixture of 30% blast furnace slag and 70% CRS powders is alkali-activated by mixing with different alkaline activating solutions of water, sodium hydroxide and sodium silicate. The viscosities and compressive strengths of the resulting inorganic binders are measured and compared with each other. Furthermore, the inorganic binder paste that has the maximum compressive strength and best workability is mixed with various amounts of preformed air bubbles to produce foamed reservoir sludge inorganic polymer (FRSIP) specimens with different densities. The effects of density on the water absorption, pore size distribution, compressive strength, bending strength and transmission loss of the FRSIP specimens are evaluated.

1. Introduction

Reservoir sludge dredging is a challenging task, and should be handled appropriately to ensure the safety of reservoirs and capacity of the public water supply. The reuse of the evacuated reservoir sludge is thus an important issue, in order to reduce its negative impacts on the environment. While reservoir sludge can be used as a raw material to produce lightweight aggregates and bricks [1–5], this process consumes much energy, which limits its practical use. Although reservoir sludge can also be organo-modified and employed as a water-proofing agent [6,7], this cannot be used to dispose of all of the sludge that is removed from reservoirs, and thus some other ways of reutilization are needed.

Inorganic polymers, first developed by Davidovits [8–10], are produced by mixing aluminosilicate minerals, such as metakaolin, fly ash and blast furnace slag, with an alkaline activating solution which is normally an alkali metal hydroxide and sodium silicate. Using this approach, the dissolution of Si and Al ions and the subsequent polycondensation reaction produce a dense three-dimensionally networked Si–O–Al microstructure [11,12]. The resulting material can have higher compressive strength than hardened Portland cement paste. As a result, alkali-activated inorganic polymeric binder can be used as a replacement for Portland cement in concrete. Reservoir sludge containing some aluminosilicate minerals, such as silts and smectite clays, was used as the raw material for a partial replacement of metakaolin in the production of inorganic polymers by Chen et al. [13,14]. They found that the reservoir sludge-based inorganic polymers could be used as binders in the production of mortars that had a high compressive strength and good workability.

Since metakaolin powders can be replaced by calcined reservoir sludge (CRS) powders [14], and the optimal replacement percentage of metakaolin by slag is around 30% [15], a mixture of weight fractions of 70% CRS and 30% blast furnace slag powders are employed here as the raw materials in the production of inorganic polymeric binders. While foamed inorganic polymers are typically produced using a chemical foaming method that has been described in several studies [16–18], less attention has been paid to the use of a mechanical foaming method. In this study, reservoir sludge is first calcined and then ground down to become CRS powders. The CRS and slag powders are then mixed with different alkaline activation solutions of sodium hydroxide and sodium silicate, and the viscosities and compressive strengths of the inorganic binders are measured and compared with each other. Furthermore, the resulting inorganic binder paste is mixed with different amounts of preformed air bubbles to produce foamed reservoir sludge inorganic polymer (FRSIP) specimens with various densities. The effects of density on the physical, mechanical and acoustic properties of the FRSIP specimens are also evaluated in this work. Foamed inorganic polymers with low embodied energy could become a substitute for Portland cement when producing foams for use as sound absorbing or thermal insulating materials.

* Corresponding author. Tel.: +886 6 7943211; fax: +886 6 2358542.
E-mail address: jshuang@mail.ncku.edu.tw (J.-S. Huang).

0958-9465/$ - see front matter © 2013 Elsevier Ltd. All rights reserved.
http://dx.doi.org/10.1016/j.cemconcomp.2013.03.017

2. Experimental methods

2.1. Materials

The reservoir sludge particles, evacuated from the A-Ken-Tien reservoir of Kaohsiung City in Taiwan, are composed of aluminosilicate minerals, such as silts and smectite clays, and can thus be used as raw materials in the production of inorganic polymers. First, the reservoir sludge particles were crushed to pass through a 300 μm sieve by using an upright pulverizer, and then further ground down using an air-isolating powder grinder. The ground reservoir sludge powders should be calcined at high temperatures to partially distort or destroy their crystalline structures in a dehydroxylation reaction before they are alkali-activated. Therefore, the reservoir sludge powders were calcined at a temperature of 850 °C for 6 h, as suggested by Chen et al. [13], and then they became more reactive, and thus the resulting alkali-activated reservoir-sludge inorganic polymers had a higher compressive strength. The main chemical compositions of the CRS powders with a specific surface area of 6740 cm^2/g employed here are 53.5% SiO_2 , 22.3% Al_2O_3 and 8.6% Fe_2O_3. In addition, blast furnace slag powders with a specific gravity of 2.9 and a chemical composition of 41.6% CaO, 34.0% SiO_2 and 13.6% Al_2O_3, supplied by China Hi-Ment Corporation in Taiwan, were employed to enhance the workability of the inorganic binder paste. Since the dissolution of the Si and Al ions of slag powders during the alkali-activation reaction of an inorganic binder depends on their fineness, powders with two different specific surface areas were used: 4180 cm^2/g, denoted by S4000, and 5810 cm^2/g, by S6000.

2.2. Alkaline activating solution and inorganic binder

A mixture of 70% CRS and 30% slag powders was alkali-activated by mixing with various alkaline activating solutions to produce inorganic binder pastes. The alkaline activating solutions are normally composed of water, sodium hydroxide and sodium silicate with a chemical composition of 25.0% SiO_2 and 8.7% Na_2O. The chemical reaction, microstructure and properties of an inorganic binder are affected significantly by the amounts of Na_2O, SiO_2 and water in the alkaline activating solution. The alkali-equivalent content, silicate modulus and water/binder ratio are generally modified in order to change the resulting material properties. The alkali-equivalent content, *AE%*, is the weight fraction of Na_2O to total powders while the silicate modulus, *Ms*, is the molar ratio of SiO_2 and Na_2O in the alkaline activating solution. The water/binder ratio, *W*/*B*, is the weight ratio of water to the sum of CRS and slag powders, SiO_2 and Na_2O.

The compressive strengths of inorganic binders produced by mixing 70% CRS and 30% slag powders with various alkaline activating solutions with different ranges of *W*/*B* = 0.25–0.5, *AE%* = 6–15% and *Ms* = 0.75–1.5 were measured by Chen et al. [14]. They confirmed that the maximum compressive strength of inorganic binders can be obtained when CRS powders are mixed with the alkaline activating solution of *W*/*B* = 0.5, *AE%* = 9% and *Ms* = 1.0. When inorganic binder paste is mixed with preformed air bubbles during the preparation of FRSIP specimens, its workability is crucial to the ease of stirring and resulting microstructure, depending on the values of *W*/*B*, *AE%* and *Ms* in the alkaline activating solution. In addition, the dissolution of the *Si* and Al ions in the slag powders is affected significantly by their fineness, leading to inorganic binder paste with different workabilities. When both the compressive strength and workability of the inorganic binders are of concern, an optimal alkaline activating solution is preferred, and should be determined experimentally. Therefore, S4000 slag powders were mixed with various alkaline activating solutions of *AE%* = 3%, 6%, 9%, 12% and 15%, *Ms* = 1.0, and *W*/*B* = 0.4 and 0.5 to produce inorganic binder pastes.

The amounts of water, sodium hydroxide and sodium silicate required for each alkaline activating solution were weighed, mixed and then placed in a container at room temperature for 1 day. CRS powders were first mixed with an alkaline activating solution and stirred vigorously for 30 min. Next, slag powders were added to the container, and this mixture was stirred for an additional 5 min to produce inorganic binder pastes. Furthermore, the variations in the viscosities with respect to time for inorganic binder pastes with the same *AE%* = 9% and *Ms* = 1.0 but different *W*/*B* were measured by using a Brookfield DVII viscometer, and then compared with each other to evaluate the effects of *W*/*B* of alkaline activating solutions and fineness of slag powders. The inorganic binder pastes were then poured into 3 cm × 3 cm × 3 cm cubic steel molds, removed from the moulds the next day and then cured in air. The 7-day, 28-day and 91-day compressive strengths of the inorganic binders were measured using a universal testing machine under a constant compressive rate of 350 KPa/s. Based on the experimental results, the optimal alkaline activating solution that produces the maximum compressive strength of inorganic binders is determined.

2.3. FRSIP specimens

Preformed air bubbles were made by stably pressurizing an aqueous solution of a foaming agent with water in a foam generating tank, and then further mixing this with the inorganic binder pastes to produce FRSIP specimens. Since the complete mixing of preformed air bubbles with inorganic binder paste depends on the *W*/*B*, two water/binder ratios of *W*/*B* = 0.4 and 0.5 were studied. The design density of each FRSIP specimen was controlled by changing the amount of preformed air bubbles introduced into the mixer, and four different densities of 0.7, 0.8, 0.9 and 1.0 g/cm^3 were considered. In addition to the amount of preformed air bubbles required for each FRSIP specimen, about 20% more than this was added because of the collapse and volume instability of the bubbles during stirring. After complete mixing of the preformed air bubbles and inorganic binder paste, the resulting FRSIP slurry was poured into steel moulds of 10 cm × 10 cm × 10 cm for compression tests and of 75 mm × 75 mm × 400 mm for bending tests. The FRSIP specimens were removed from the steel moulds next day and cured in air at room temperature. The 7-day, 28-day and 91-day compressive and bending strengths of the FRSIP specimens were measured by conducting a series of compression and bending tests in a universal testing machine.

The actual densities of the FRSIP specimens and solid inorganic binders were measured and recorded before mechanical testing. In addition, the water absorption levels of the FRSIP specimens with different densities were measured and then compared with each other to evaluate the effects of density. Images of cross-sections of the FRSIP specimens were taken using a digital camera, and the pore size distributions within them were analyzed using the image analysis software in Matlab. FRSIP specimens with different densities of 0.7, 0.8, 0.9 and 1.0 g/cm^3 but the same dimensions of 60 cm × 60 cm × 10 cm and 60 cm × 60 cm × 6 cm were prepared for acoustic testing. The transmission losses of the FRSIP specimens were measured according to the standard method of ISO 15168, and compared with those of commercially available gypsum, cement and calcium silicate boards with dimensions of 60 cm × 60 cm × 10 cm, which are widely used as noise-protection materials in Taiwan.

3. Results and discussion

3.1. Viscosity of inorganic binder paste

After mixing the CRS powders, alkaline activating solution and slag powders with a fineness of S4000 or S6000 for 35 min, the

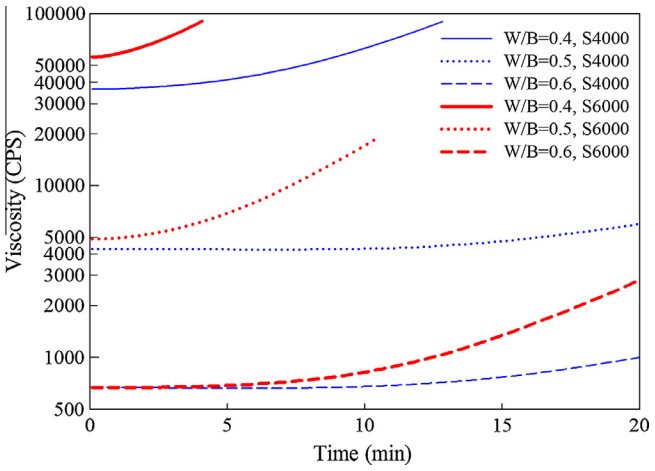

Fig. 1. Variation of viscosities with respect to time for inorganic binder pastes with various water/binder ratios and two finenesses of slag powders.

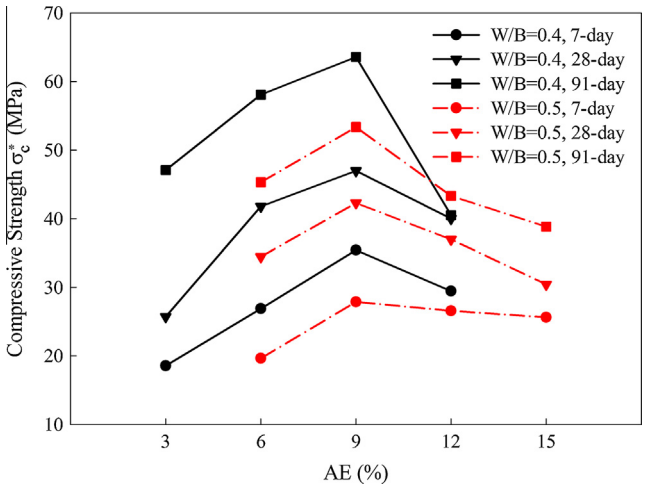

Fig. 2. The 7-day, 28-day and 91-day compressive strengths of inorganic binders alkali-activated by mixing with alkaline activating solutions of different *W*/*B* and *AE*%.

viscosities of each inorganic binder paste were measured and recorded continuously for 20 min. The variations of the viscosities of inorganic binder pastes, with the same *AE*% = 9% and *Ms* = 1.0 but different *W*/*B* = 0.4, 0.5 and 0.6, are shown in Fig. 1. It can be seen that the viscosities of all the inorganic binder pastes increased steadily with respect to time, regardless of the water/binder ratio in an alkaline activating solution and the fineness of slag powders. The viscosities of the inorganic binder pastes with *W*/*B* = 0.4 are much greater than those with *W*/*B* = 0.5 and 0.6 at any time. In addition, the viscosities of the inorganic binder pastes with S6000 slag powders are consistently larger than those with same *W*/*B* but made with S4000 slag powders. Therefore, the viscosity of an inorganic binder paste can be increased dramatically when the water/binder ratio of the alkaline activating solution is reduced, or the specific surface area of slag powders is increased.

When preformed air bubbles are mixed with an alkaline activating solution, viscosities of less than 5000 CPS in the resulting inorganic binder paste are preferred for the first 20 min of stirring. If the viscosity is greater than this, it is difficult to stir in a mixer, and the collapse and destruction of the preformed air bubbles are more likely to occur, leading to a less dense microstructure and lower compressive strength. In Fig. 1, the starting viscosities are much greater than 5000 CPS for the inorganic binder pastes with *W*/*B* = 0.4. In contrast, the viscosities of the inorganic binder pastes with *W*/*B* = 0.6 are around 700 CPS at the beginning, and then still less than 3000CPS even 20 min later. In other words, the reaction rate of dissolution is higher than that of polycondensation for the first 5–10 min of stirring, providing a lower viscosity that is beneficial to the mixing of the preformed air bubbles and inorganic binder paste. However, the viscosities increase steadily when the stirring time is more than 10 min, because the polycondensation reaction rate becomes faster than the dissolution reaction rate. Fig. 1 shows that the three inorganic binder pastes of *W*/*B* = 0.6 and S4000, *W*/*B* = 0.6 and S6000, and *W*/*B* = 0.5 and S4000 are all good candidate materials for mixing with preformed air bubbles to produce FRSIP specimens.

3.2. Optimal alkaline activating solution

The compressive strengths of inorganic binders depend on the water/binder ratio, the alkali-equivalent content in the alkaline activating solutions, and the curing time. The 7-day, 28-day and 91-day compressive strengths of the inorganic binders produced by mixing S4000 slag powders with various alkaline activating solutions of *Ms* = 1.0, *AE*% = 3%, 6%, 9%, 12% and 15%, and *W*/*B* = 0.4 and 0.5 are presented in Fig. 2. It can be seen that the compressive strengths of the inorganic binders with *W*/*B* = 0.4 are higher than those with *W*/*B* = 0.5, and that they increase along with the curing time. Meanwhile, the compressive strengths of the inorganic binders increase steadily at the beginning and then drop significantly after reaching a maximum at *AE*% = 9%, as the alkali-equivalent content is increased from 3% to 15%, regardless of *W*/*B* and the curing time. Therefore, the optimal alkaline activating solution that produces the maximum compressive strength of inorganic binders is that with *W*/*B* = 0.5, *AE*% = 9% and *Ms* = 1.0, when both their viscosity and compressive strength are of interest.

3.3. Microstructure of FRSIP specimens

It is known that the water absorption of a porous solid is related to its total porosity and the morphology of the interfacial area between any adjacent connected air bubbles. Therefore, the water absorption capacity can be used to represent the microstructure and total volume of air bubbles within each FRSIP specimen. The water absorption of the FRSIP specimens with various design densities of 0.7, 0.8, 0.9 and 1.0 g/cm^3 are plotted in Fig. 3. It is seen that the water absorption of the FRSIP specimens decreases steadily with increasing design density, due to the reduction in the

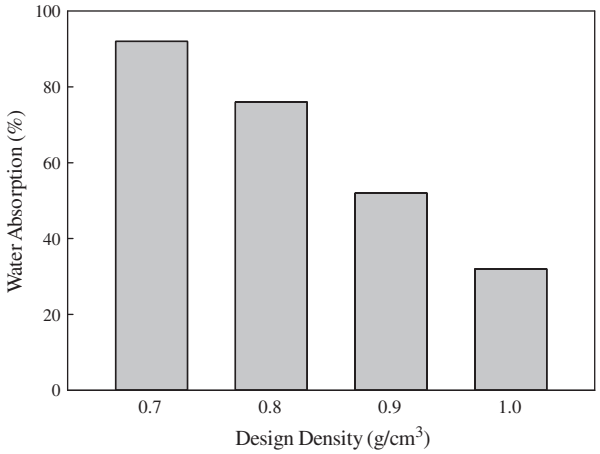

Fig. 3. Variation of the water absorptions of the FRSIP specimens with different design densities of 0.7, 0.8, 0.9 and 1.0 g/cm^3.

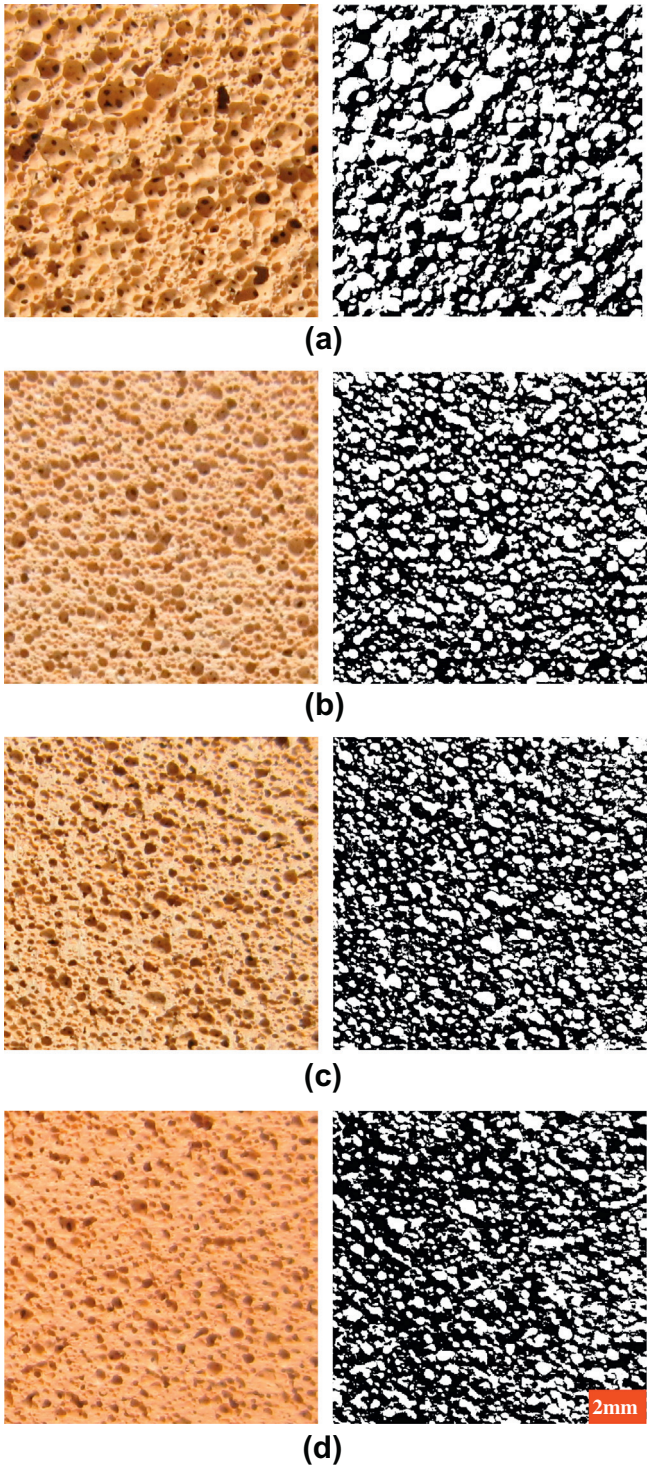

Fig. 4. The original and darkened images of the cross-sections of the FRSIP specimens with a water/binder ratio of 0.5 and different design densities of: (a) 0.7 g/cm^3, (b) 0.8 g/cm^3, (c) 0.9 g/cm^3, and (d) 1.0 g/cm^3 .

total volume of air bubbles. The water absorption can reach up to 90% when the density is reduced to 0.7 g/cm^3.

The microstructures of FRSIP specimens were further characterized by analyzing the pore size distributions within them using the image analysis software in Matlab. The original and darkened images of the cross-sections parallel to the direction of gravity of the FRSIP specimens with a design density of 0.7, 0.8, 0.9 and 1.0 g/cm^3 are shown in Fig. 4a–d respectively when $W/B = 0.5$.

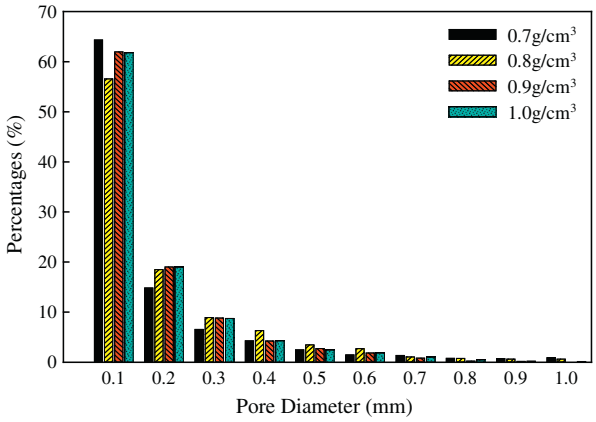

Fig. 5. The pore size distributions of the FRSIP specimens with a water/binder ratio of 0.5 and different design densities of 0.7, 0.8, 0.9 and 1.0 g/cm^3.

The measured pore size distributions of the FRSIP specimens are plotted in Fig. 5, and it can be seen that more than 80% of the pores in the FRSIP specimens are less than 0.3 mm. Since the density of an FRSIP specimen is controlled by changing the amount of preformed air bubbles introduced into the mixture, the resulting pore size distribution depends on the amount of bubbles. The results show that the pore size distributions of the FRSIP specimens are almost identical, as expected. Therefore, it can be said that effect of density on the pore size distribution is insignificant.

3.4. Compressive and bending strengths of FRSIP specimens

The actual densities, compressive strengths and bending strengths of the FRSIP specimens with design densities of 0.7, 0.8, 0.9 and 1.0 g/cm^3 were measured, recorded and then compared with each other. The relative density of each FRSIP specimen is the ratio of its actual density, ρ^*, to that of solid inorganic binder, ρ_s. The measured 7-day, 28-day and 91-day compressive strengths of the FRSIP specimens, σ_C^*, are plotted against their relative densities, ρ^*/ρ_s, in a log–log scale in Fig. 6a–c, respectively. The compressive strengths increase with increasing relative density, and can be described by the following equation derived by Gibson and Ashby [19] from a cell-edge bending model for lower relative-density foams:

$$\sigma_C^* = C_1 \sigma_{CS} \left(\frac{\rho^*}{\rho_s} \right)^m \tag{1}$$

Here, σ_{CS} is the compressive strength of the solid inorganic binder, and the two microstructural coefficients, C_1 and m, should be experimentally determined. By conducting a series of regression analyses on the experimental results shown in Fig. 6, the exponential constants $m = 2.37$, 2.15 and 2.57 are obtained for the 7-day, 28-day and 91-day compressive strengths of the FRSIP specimens, respectively. The measured exponential constants are within the range of 1.5 for low relative-density foams given in Gibson and Ashby [19] and 4.0 for porous solids suggested by Roy and Gouda [20]. Since the variations of the compressive strengths in Fig. 6 and the pore size distributions in Fig. 5 are insignificant, it can be concluded that the preformed air bubbles in the FRSIP specimens introduced by employing a mechanical foaming method are distributed randomly and uniformly.

In a similar way, the 7-day, 28-day and 91-day bending strengths of the FRSIP specimens, σ_B^*, increase with increasing relative density, as shown in Fig. 7a–c respectively, and can be described by the following equation:

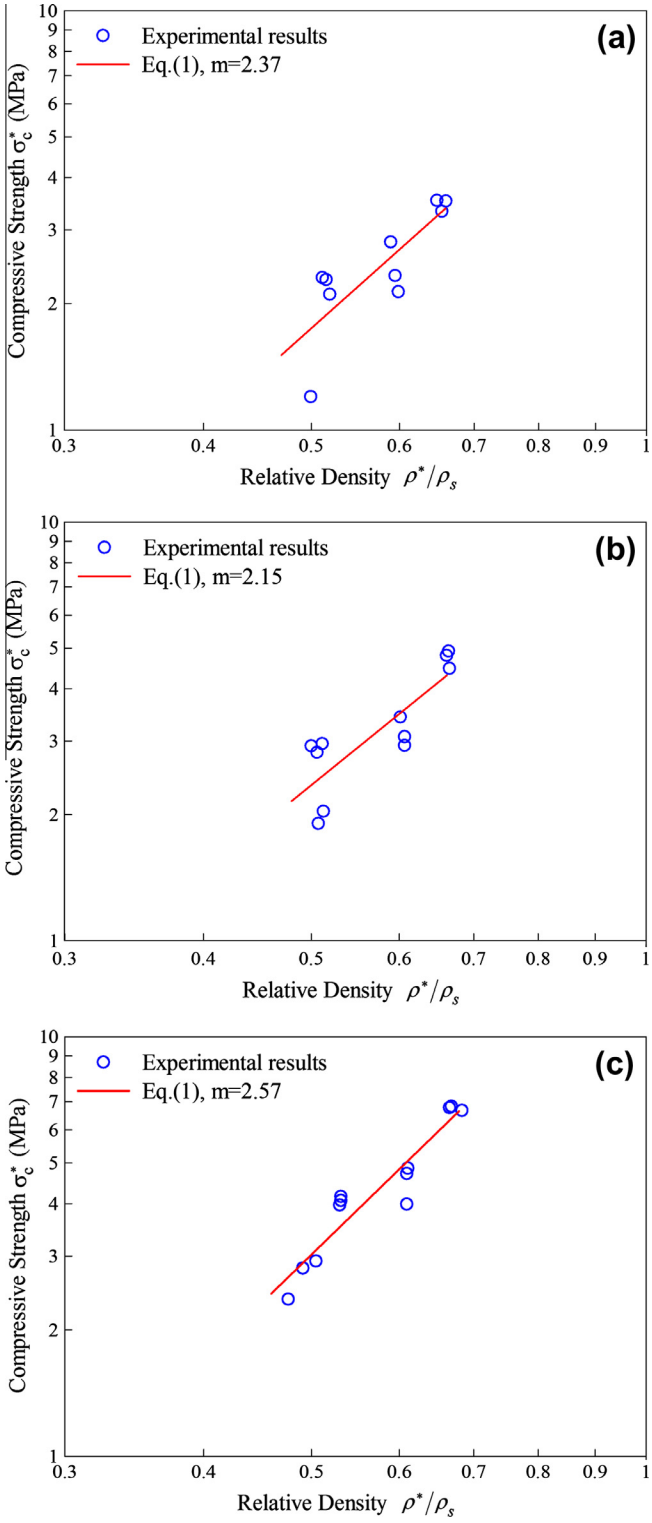

Fig. 6. The (a) 7-day (b) 28-day and (c) 91-day compressive strengths of the FRSIP specimens with same $W/B = 0.5$ but different design densities.

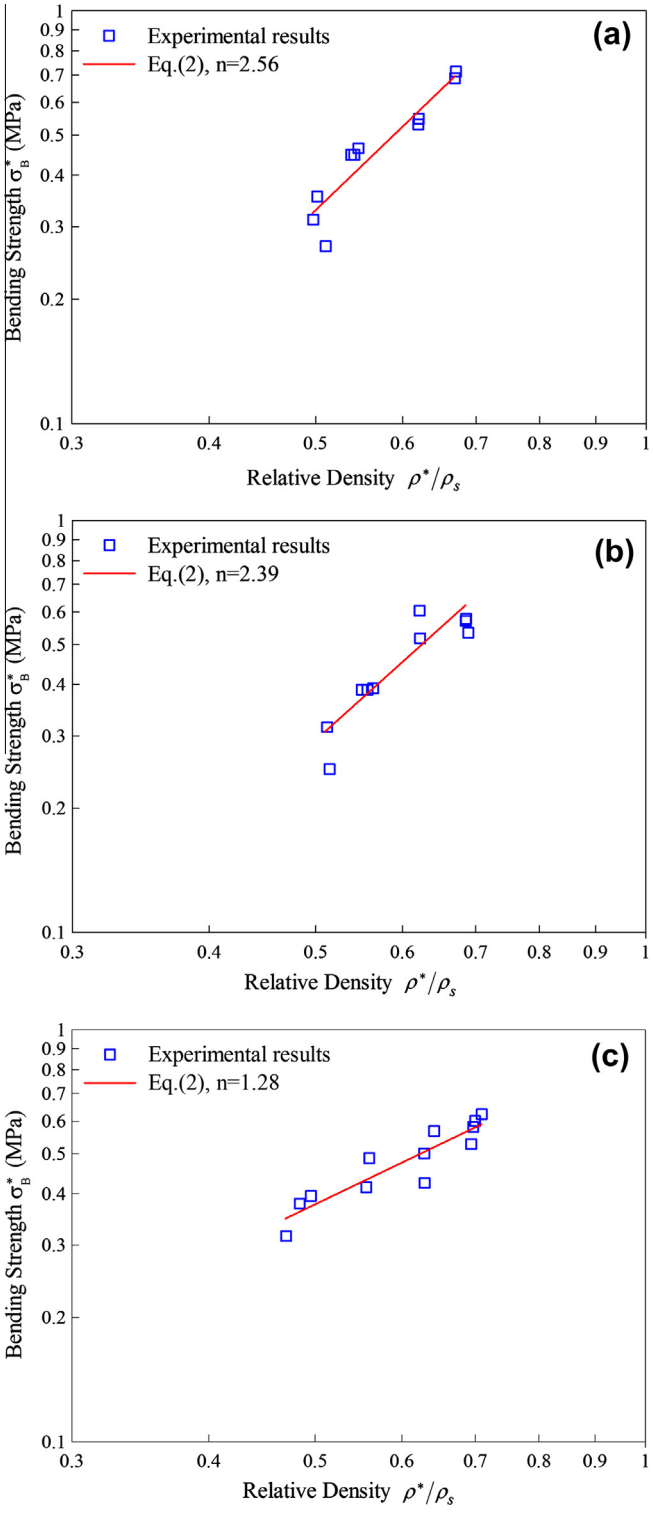

Fig. 7. The (a) 7-day (b) 28-day and (c) 91-day bending strengths of the FRSIP specimens with same $W/B = 0.5$ but different design densities.

$$\sigma_B^* = C_2 \sigma_{BS} \left(\frac{\rho^*}{\rho_s}\right)^n \tag{2}$$

In Eq. (2), σ_{BS} is the bending strength of solid inorganic binders, and the two microstructural coefficients, C_2 and n, should again be determined experimentally. The exponential constants $n = 2.56$, 2.39 and 1.28 are obtained from a series of regression analyses on the 7-day, 28-day and 91-day bending strengths of the FRSIP specimens shown in Fig. 7, respectively.

From Figs. 6 and 7, it is noted that the variation of bending strengths is slightly larger than that of the compressive strengths, because the former are more sensitive to the maximum-size crack within each FRSIP specimen. For comparison, the compressive strengths of the FRSIP specimens are plotted against their

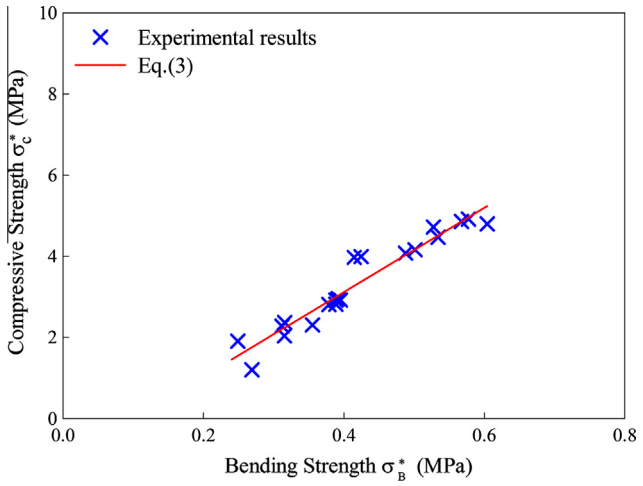

Fig. 8. Comparison between compressive strengths and bending strengths of the FRSIP specimens with same $W/B = 0.5$ but different design densities.

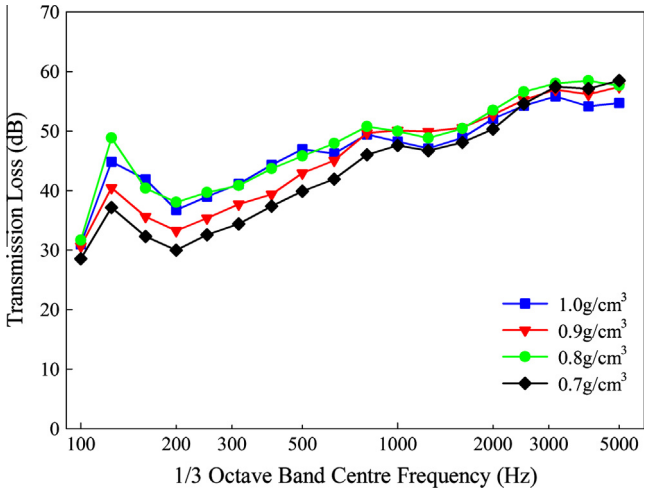

Fig. 9. The transmission losses of the FRSIP specimens with same thickness of 6 cm but different design densities.

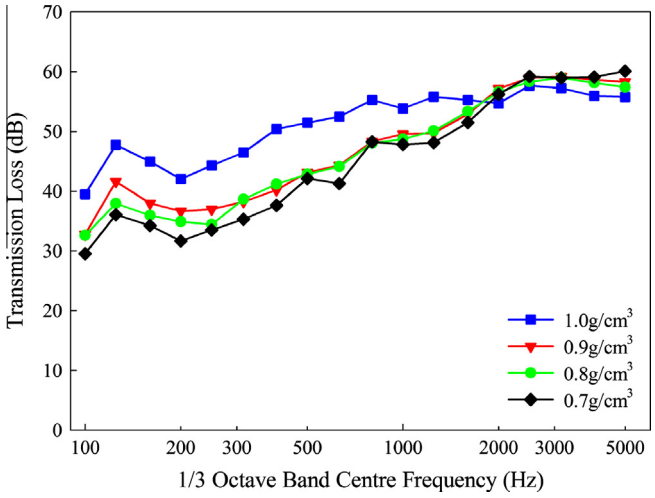

Fig. 10. The transmission losses of the FRSIP specimens with same thickness of 10 cm but different design densities.

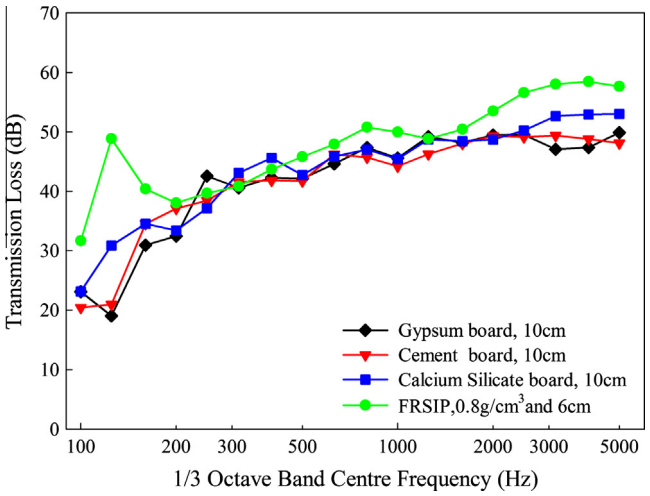

Fig. 11. Comparison of the transmission losses of commercially available gypsum, cement and calcium silicate boards with a thickness of 10 cm, and the FRSIP specimen with a design density of 0.8 g/cm^3 and a thickness of 6 cm.

corresponding bending strengths in Fig. 8. Based on the experimental results in Fig. 8, the following relationship between compressive strength and bending strength can be obtained from a regression analysis:

$$\sigma_C^* = 10.4\sigma_B^* - 1.04\ \text{MPa} \quad (3)$$

It can thus be said that the compressive strength of a FRSIP specimen is roughly 10 times its bending strength.

3.5. Transmission losses of FRSIP specimens

The transmission losses of the FRSIP specimens with a thickness of 6 cm but different densities are presented in Fig. 9. It is seen that the transmission losses of the FRSIP specimens with a design density of 0.8 g/cm^3 are higher than those of 0.7, 0.9 and 1.0 g/cm^3 when frequency is within the range of 100–1000 Hz. The difference between the transmission losses of the FRSIP specimens is less than 4 dB, and becomes insignificant when the frequency is larger than 1000 Hz. When the thickness is increased to 10 cm, as shown in Fig. 10, the transmission losses of the FRSIP specimens increase with increasing density when the frequency is less than 2000 Hz, but become independent of density when it is higher than 2000 Hz. In other words, the transmission losses of the FRSIP specimens can be described by the well-known mass law if their thicknesses become equal to or thicker than 10 cm. Based on the experimental results in Figs. 9 and 10, it can be concluded that the transmission losses of the FRSIP specimens are affected by their density and thickness, and thus their surface density, which is the product of these. Furthermore, the transmission losses of the FRSIP specimen with a design density of 0.8 g/cm^3 and a thickness of 6 cm are compared with those of gypsum, cement and calcium silicate boards with a thickness of 10 cm, as shown in Fig. 11, and it can be seen that a thinner FRSIP specimen provides better noise protection than a thicker gypsum, cement or calcium silicate board.

4. Conclusions

Based on the experimental results, the findings of the work can be summarized as follows.

1. The viscosities of inorganic binder pastes increase significantly when the water/binder ratio of alkaline activating solutions and the size of slag powders are reduced.
2. The alkaline activating solution that produces the maximum compressive strength of inorganic binders is $W/B = 0.5$, $AE\% = 9\%$ and $Ms = 1.0$.
3. The water absorption of the FRSIP specimens increases as the density decreases, and it can be up to 90% when the density is reduced to 0.7 g/cm^3.
4. More than 80% of the pores within the FRSIP specimens are less than 0.3 mm in diameter, and the effect of their density on the pore size distribution within them is insignificant.
5. The compressive and bending strengths of the FRSIP specimens increase with increasing relative density.
6. The transmission losses of the FRSIP specimens are affected by their density and thickness.
7. The transmission losses of the FRSIP specimen with 0.8 g/cm^3 and a thickness of 6 cm are superior to those of gypsum, cement and calcium silicate boards with a thickness of 10 cm.

Acknowledgement

The financial support of the National Science Council, Taiwan, ROC, under Contract Number NSC 99-2221-E-006-184-MY3 is gratefully acknowledged.

References

[1] Chen H-J, Yang M-D, Tang C-W, Wang S-Y. Producing synthetic lightweight aggregates from reservoir sediments. Constr Build Mater 2012;28(1):387–94.
[2] Tang C-W, Chen H-J, Wang S-Y, Spaulding J. Production of synthetic lightweight aggregate using reservoir sediments for concrete and masonry. Cem Concr Compos 2011;33(2):292–300.
[3] Chiang K-Y, Chien K-L, Hwang S-J. Study on the characteristics of building bricks produced from reservoir sediment. J Hazard Mater 2008;159(2–3):499–504.
[4] Liao Y-C, Huang C-Y. Glass foam from the mixture of reservoir sediment and Na_2CO_3. Ceram Int 2012;38(5):4415–20.
[5] Liao Y-C, Huang C-Y. Effects of CaO addition on lightweight aggregates produced from water reservoir sediment. Constr Build Mater 2011;25(6):2997–3002.
[6] Kuo W-Y, Huang J-S, Tan T-E. Organo-modified reservoir sludge as fine aggregates in cement mortars. Constr Build Mater 2007;21(3):609–15.
[7] Kuo W-Y, Huang J-S. Microstructure and properties of cement mortars containing organo-modified reservoir sludge. Constr Build Mater 2010;24(10):2022–9.
[8] Davidovits J. Early high-strength mineral polymer. United States patent 4509985; 1985.
[9] Davidovits J. Mineral polymers and methods of making them. United States patent 4349386; 1982.
[10] Davisovits J. Geopolymers: inorganic polymeric new materials. J Therm Anal 1991;37(8):1633–56.
[11] Xu H, Van Deventer JSJ. Geopolymerisation of multiple minerals. Miner Eng 2002;15(12):1131–9.
[12] Xu H, Van Deventer JSJ. The geopolymerisation of alumino-silicate minerals. Int J Miner Process 2000;59(3):247–66.
[13] Chen JH, Huang JS, Chang YW. A preliminary study of reservoir sludge as a raw material of inorganic polymers. Constr Build Mater 2009;23(10):3264–9.
[14] Chen J-H, Huang J-S, Chang Y-W. Use of reservoir sludge as a partial replacement of metakaolin in the production of geopolymers. Cem Concr Compos 2011;33(5):602–10.
[15] Davidovits J, Davidovits R, James C. Chemistry of geopolymeric systems terminology. In: Proc. of geopolymer 99 sec. international conf; 1999. p. 9–37.
[16] Schmidt G, Randel P, Engels H-W, Geick B. Furnace with in situ foamed insulation and process for its manufacture. United States patent 5485986; 1996.
[17] Arellano Aguilar R, Burciaga Díaz O, Escalante García JI. Lightweight concretes of activated metakaolin-fly ash binders, with blast furnace slag aggregates. Constr Build Mater 2010;24(7):1166–75.
[18] Esmaily H, Nuranian H. Non-autoclaved high strength cellular concrete from alkali activated slag. Constr Build Mater 2012;26(1):200–6.
[19] Gibson LJ, Ashby MF. Cellular solids: structures and properties. 2nd ed. Cambridge UK: Cambridge University Press; 1997.
[20] Roy DM, Gouda GR. Porosity-strength relation in cementitious materials with very high strengths. J Am Ceram Soc 1973;56(10):549–50.